3060 *Chem. Mater.* **2010,** *22,* 3060–3066
DOI:10.1021/cm903636j

CHEMISTRY OF MATERIALS
Article

Direct-Liquid-Injection Chemical Vapor Deposition of Nickel Nitride Films and Their Reduction to Nickel Films

Zhefeng Li,[†] Roy G. Gordon,*[,†] Venkateswara Pallem,[†,‡] Huazhi Li,[§] and Deo V. Shenai[§]

[†]*Department of Chemistry and Chemical Biology, Harvard University, Cambridge, Massachusetts 02138,* and [§]*Dow Electronic Materials, North Andover, Massachusetts 01845.* [‡]*Current address: Air Liquide, Newark, DE 19702.*

Received December 1, 2009. Revised Manuscript Received April 5, 2010

Smooth and continuous films of nickel nitride (NiN_x) with excellent step coverage were deposited from a novel nickel amidinate precursor, $Ni(MeC(N^tBu)_2)_2$, and either ammonia (NH_3) or a mixture of NH_3 and hydrogen (H_2) gases as co-reactants. The reactants were injected together in direct-liquid-injection chemical vapor deposition (DLI-CVD) processes at substrate temperatures of 160−200 °C. Depending on the ratio of NH_3 to H_2 gases during deposition, the Ni:N atomic ratio in DLI-CVD NiN_x films could be varied from ~3:1 to ~15:1, having either a cubic nickel structure or a mixture of hexagonal Ni_3N and cubic Ni_4N crystal structures with an incorporation of nitrogen as low as 6%. The chemical vapor deposition (CVD) growth rates of NiN_x could be increased to more than 5 nm/min. The CVD films were smooth and continuous, and they had ~100% step coverage in high-aspect-ratio (> 50:1) holes. The as-deposited NiN_x films had resistivities as low as ~50 $\mu\Omega$ cm for film thicknesses of ~25 nm. Annealing of the films in H_2 at 160 °C or hydrogen plasma treatment at room temperature removed the nitrogen and led to pure nickel films.

Introduction

Nickel has received considerable attention in microelectronic applications, because it can react with silicon to form nickel monosilicide (NiSi), which is becoming the key material for source and drain contacts in semiconductor device processing for the 65-nm technology node and beyond.[1] NiSi has the advantage of a lower temperature of formation and lower silicon consumption to obtain the same sheet resistance, compared to the other two most commonly used silicides: $TiSi_2$ and $CoSi_2$.[2] Fully silicided (FUSI) Ni gates also can replace poly-Si gates in complementary metal−oxide silicon (CMOS) devices.[3] Nickel films have also been used as protective coatings against oxidation and corrosion, and as decorative and selective absorbers.[4] Other applications of nickel include use as fuel cells[5] and catalysts.[6]

Nickel films have been deposited by various methods, including sputtering, chemical vapor deposition (CVD), and atomic layer deposition (ALD).[7] As the dimensions of microelectronic circuits are being reduced, sputtering cannot provide a uniform film thickness inside the narrow features needed in future microelectronic devices,[8] such as nanoscale CMOS devices or three-dimensional MOS devices such as Fin-type field-effect transistors (Fin-FETs).[9] CVD and ALD are considered to produce more-conformal nickel films. Nickel films have been prepared by metal−organic chemical vapor deposition (MOCVD) methods, using precursors such as nickel carbonyl $Ni(CO)_4$, bis(cyclopentadienyl)nickel $Ni(C_5H_5)_2$,[10] nickel β-diketonates (such as nickel(II) acetylacetonate $Ni(acac)_2$ or bis(2,2,6,6-tetramethyl-3,5-heptanedionato)nickel(II) $Ni(TMHD)_2$),[11] etc. However, these precursors suffer from either poor thermal stability, causing degradation of the precursor and incorporation of carbon into the films, or low vapor pressure, leading to poor step coverage in high-aspect-ratio structures. ALD is an attractive deposition technique for forming thin and continuous thin films with excellent step coverage.[12] So far, there have been few reports on the ALD of nickel films. Most of the processes reported for the ALD of nickel films

*Author to whom correspondence should be addressed. E-mail: gordon@chemistry.harvard.edu.

(1) Foggiato, J.; Yoo, W. S.; Ouaknine, M.; Murakami, T.; Fukada, T. *Mater. Sci. Eng., B* **2004**, *114*−*115*, 56.
(2) Chen, L. J. *Silicide Technology for Integrated Circuits*; Institute of Electrical Engineers (IEE): London, 2004.
(3) Kittl, J. A.; Lauwers, A.; Hoffmann, T.; Veloso, A.; Kubicek, S.; Niwa, M.; van Dal, M. J. H.; Pawlak, M. A.; Demeurisse, C.; Vrancken, C.; Brijs, B.; Absil, P.; Biesemans, S. *IEEE Elect. Device Lett.* **2006**, *27*(8), 647.
(4) Premkumar, P. A.; Dasgupta, A.; Kuppusami, P.; Parameswaran, P.; Mallika, C.; Nagaraja, K. S.; Raghunathan, V. S. *Chem. Vap. Deposition* **2006**, *12*, 39.
(5) Morse, J. D.; Jankowski, A. F.; Graff, R. T.; Hayes, J. P. *J. Vac. Sci. Technol. A* **2000**, *18*(4), 2003.
(6) Golikand, A. N.; Asgari, M.; Maragheh, M. G.; Shahrokhian, S. *J. Electroanal. Chem.* **2006**, *588*(1), 155.
(7) Pauleau, Y.; Kukielka, S.; Gulbinski, W.; Ortega, L.; Dub, S. N. *J. Phys. D: Appl. Phys.* **2006**, *39*, 2803.
(8) The International Technology Roadmap for Semiconductors; Available via the Internet at http://public.itrs.net, accessed **2007**.
(9) Huang, X. J.; Lee, W. C.; Kuo, C.; Hisamoto, D.; Chang, L.; Kedzierski, J.; Anderson, E.; Takeuchi, H.; Choi, Y. K.; Asano, K.; Subramanian, V.; King, T. J.; Bokor, J.; Hu, C. M. *IEEE Trans. Elect. Dev. Lett.* **2001**, *48*(5), 880.
(10) Brissonneau, L.; Vahlas, C. *Chem. Vap. Deposition* **1999**, *5*(4), 135.
(11) Bahlawane, N.; Premkumar, P. A.; Onwuka, K.; Reiss, G.; Kohse-Hoinghaus, K. *Microelectron. Eng.* **2007**, *84*(11), 2481.
(12) Gordon, R. G.; Hausmann, D.; Kim, E.; Shepard, J. *Chem. Vap. Deposition* **2003**, *9*(2), 73.

Published on Web 04/27/2010

employed the deposition of nickel oxide and the subsequent reduction of the oxide to nickel by annealing the films under molecular hydrogen or hydrogen radical atmosphere.[13,14] However, the reduction of such oxide films to nickel induces high-volume shrinkage, affecting the morphology and continuity of the reduced films. For example, volume shrinkage from the reduction of bunsenite (NiO) (bulk density: 6.67 g/cm^3) to cubic nickel (bulk density: 8.90 g/cm^3) is ~41%. It was found that the reduction step did induce structural collapse and pinhole formation. Oxygen and carbon were left inside the films after reduction, which increases the resistivity of the nickel films. For the purpose of forming nickel silicides from such reduced nickel films deposited on silicon, the oxygen content inside the films could oxidize the silicon interface, impeding silicide formation and causing agglomeration of the silicide films during heat treatment. Our group had previously deposited nickel films by reducing the precursor bis(*N*,*N*′-diisopropylacetamidinato)nickel(II), Ni(MeC(N^{i}Pr)$_2$)$_2$, with molecular H_2.[15] However, this precursor partially decomposed after heating in a bubbler for several days and the ALD growth rate of nickel films, using this precursor, was also too low (~0.04 Å/cycle) for many applications.

Direct-liquid-injection chemical vapor deposition (DLI-CVD) is a very attractive deposition method that is applicable to a very wide range of precursors,[16] especially for those having low vapor pressure. DLI-CVD with suitable liquids or solutions can consistently deliver high vapor concentrations of precursors that are very difficult to achieve by vaporization from conventional bubblers. Higher vapor concentrations can deposit highly conformal films with high growth rates. In the present work, we employed a novel metal−organic precursor, bis(*N*,*N*′-di-*tert*-butylacetamidinato)nickel(II), Ni(MeC(N^{t}Bu)$_2$)$_2$, which is much more thermally stable than the precursor mentioned above, Ni(MeC(N^{i}Pr)$_2$)$_2$, for DLI-CVD processes. Instead of direct reduction with H_2 or forming nickel oxide with subsequent reduction, we deposited nickel nitride (NiN_x) as an intermediate film using NH_3 or a mixture of NH_3/H_2 gases as co-reactants. It has been reported that nickel nitride phases decompose to pure nickel at high temperatures.[17] In this work, we found that NiN_x can be reduced to pure nickel metal by hydrogen at temperatures of 160 °C, or by remote hydrogen plasma at room temperature. The reduction of NiN_x films to pure nickel only induces a smaller volume shrinkage. For example, the volume shrinkages from the reduction of hexagonal Ni_3N and cubic Ni_4N to cubic nickel are 20.1% and 17.0%, respectively, which are about half the shrinkage during the reduction of nickel oxide.

We found that the DLI-CVD of NiN_x using Ni(MeC(N^{t}Bu)$_2$)$_2$ with NH_3 as the co-reactant formed films with a mixture of hexagonal Ni_3N and cubic Ni_4N crystal structures with a N:Ni atomic ratio of up to 1:3. DLI-CVD of NiN_x with a mixture of NH_3/H_2 gases as the co-reactant formed cubic Ni_4N or Ni phases with as little as 6% nitrogen incorporation, depending on the NH_3:H_2 ratio. By suitable optimization of the deposition conditions, the DLI-CVD films can be made as conformal as ALD films, but in a much shorter deposition time. The films were either annealed in situ in hydrogen at 160 °C or treated with H_2 plasma at room temperature to yield pure nickel films without agglomeration. Both methods led to similar results, as evidenced by sheet resistance measurements. We report elsewhere[18] that NiN_x films on silicon can be annealed to form pure NiSi with excellent properties.

Experimental Section

The precursor for the nickel film deposition is bis(*N*,*N*′-di-*tert*-butylacetamidinato)nickel(II), Ni(MeC(N^{t}Bu)$_2$)$_2$. All reactions and manipulations for the synthesis of Ni(MeC(N^{t}Bu)$_2$)$_2$ were conducted under a pure nitrogen atmosphere, using either an inert atmosphere box or Schlenk techniques. Tetrahydrofuran (THF) and pentanes (Aldrich Chemical Co.) were dried using an Innovative Technology solvent purification system. Methyllithium (MeLi), 1,3-di-*tert*-butylcarbodiimide, 1,3-diisopropylcarbodiimide, and nickel dichloride ($NiCl_2$) (Aldrich) were used as received.

A solution of 1,3-di-*tert*-butylcarbodiimide (10.0 g, 64.8 mmol) in 100 mL of THF at −78 °C was added to a solution of MeLi (40.5 mL, 64.8 mmol) and stirred at −78 °C for 30 min. The reaction mixture was warmed to room temperature and further stirred for 2 h. A yellow suspension of $NiCl_2$ (4.2 g, 32.4 mmol) in 150 mL of THF was added to the Li-salt solution via a cannula; the yellow suspension disappeared within few minutes, and the resulting dark brown solution was stirred for 16 h. The solvent was evaporated to dryness (60 °C); pentane (50 mL) was added and stirred for 10 min, and then again evaporated to dryness (60 °C). The resulting brown solid was extracted with pentane and filtered through a Celite pad, and the filtrate was evaporated to dryness, resulting in a dark brown solid (11.37 g, 88% yield). Sublimation: 95 °C at 50 mTorr. Mp: 87 °C. ^{1}H NMR (C_6D_6, 25 °C, ppm): 99.53 (s, 3H, CCH_3), 17.96 (s, 18H, $NC(CH_3)_3$). Anal. Calcd. for $C_{20}H_{42}N_4Ni$: C 60.47, H 10.66, N 14.10. Found: C 60.01, H 10.24, N 13.84. The crystal structure of the product is shown in Figure 1. The paramagnetic NMR spectrum is expected for the distorted tetrahedral coordination of d^8 Ni(II). For comparison, bis(*N*,*N*′-diisopropylacetamidinato)nickel(II), Ni(MeC(N^{i}Pr)$_2$)$_2$,[15] was made by a similar procedure with 1,3-diisopropylcarbodiimide in place of 1,3-di-*tert*-butylcarbodiimide.

Vapor pressure was evaluated by static vapor pressure measurement, using a heated MKS capacitance manometer. Thermogravimetric analysis (TGA) was conducted in a TA Instruments Model Q50 system inside a glovebox at a ramp rate of 10 K/min in flowing nitrogen at atmospheric pressure. Accelerated Rate Calorimetry (ARC) was performed in a system that was built by Arthur D. Little, Inc. The ARC experiment was typically run with 2 g of sample. It proceeded automatically with a heat-wait-search-exotherm mode of

(13) Chae, J.; Park, H. S.; Kang, S. W. *Electrochem. Solid State Lett.* **2002**, *5*(6), C64.
(14) Utriainen, M.; Kroger-Laukkanen, M.; Johansson, L. S.; Niinisto, L. *Appl. Surf. Sci.* **2000**, *157*(3), 151.
(15) (a) Lim, B. S.; Rahtu, A.; Gordon, R. G. *Nat. Mater.* **2003**, *2*, 749. (b) Lim, B. S.; Rahtu, A.; Park, J.-S.; Gordon, R. G. *Inorg. Chem.* **2003**, *42*, 7951.
(16) Song, M. K.; Kang, S. W.; Rhee, S. W. *Thin Solid Films* **2004**, *450*, 272.
(17) Maya, L. *J. Vac. Sci. Technol. A* **1993**, *11*(3), 604.
(18) Li, Z.; Gordon, R. G.; Li, H.; Shenai, D. V.; Lavoie, C. J. Electrochem. Soc. In press.

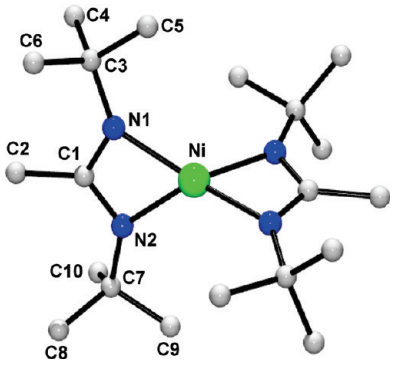

Figure 1. Crystal structure of nickel bis(*N*,*N*′-di-*tert*-butylacetamidinate).

operation, and the onset of decomposition was determined by the increase in the pressure of the volatile decomposition products.

For DLI-CVD processes, tetrahydronaphthalene (commonly called tetralin) was used to dissolve the nickel precursor. The solubility of the nickel precursor in tetralin was determined to be ~50 wt %. In this work, a 40 wt % solution of $Ni(MeC(N^tBu)_2)_2$ in tetralin was prepared and transferred into a glass container in a glovebox. The precursor solution was kept at room temperature and was pressurized by pure N_2 at a pressure of 4 bar. The flow of the precursor solution was controlled by a Horiba−Stec liquid flow controller at flow rates up to 0.1 cm^3/min. The precursor solution was mixed with N_2 carrier gas at room temperature in a tee, from which the liquid and gas flowed together into a coil of stainless steel tubing kept at 150 °C in an oven as described elsewhere.[19] The vapor mixture exiting from this tubing was mixed at a tee with H_2 and/or NH_3 reactant gases a few centimeters before entering the end of a tubular warm-wall reactor. The substrates were supported on an aluminum half-cylinder inserted into the reactor tube. A heating element and a control thermocouple were embedded in the half-cylinder under the substrates. The substrates were typically held at temperatures of 160−240 °C and heated ~10 °C higher than the wall temperature in the tube furnace. The deposition pressure was set at values of 1−10 Torr. The sum of the flow rates of NH_3 and H_2 was fixed at 60 sccm, while the flow of N_2 was set to 60 sccm.

Silicon, silicon-on-insulator (SOI), thermally oxidized silicon wafers, glassy carbon, and Si_3N_4 membranes (TEM grids from Ted Pella, Inc.) were used as substrates. Before deposition, the substrates were treated with UV/ozone to remove organic contaminants. Silicon and SOI wafers were further dipped in 5% aqueous HF solution for ~10 s to achieve a hydrogen-terminated surface.

The sheet resistance of both the as-deposited and the annealed films deposited on thermally oxidized silicon wafers was measured by a four-point probe station (Veeco Instruments, Model FPP-100, or Miller Design & Equipment, Model FPP-5000). The mass of nickel deposited was measured by Rutherford backscattering spectroscopy (RBS). The physical thickness of the CVD films was measured by X-ray reflectometry (XRR). The density of the CVD films was evaluated by combining XRR and RBS results. The nucleation and crystalline phases of both the as-deposited and the annealed films of NiN_x were evaluated by transmission electron microscopy (TEM) (JEOL Model JEL2100 TEM system), electron diffraction (ED), and X-ray diffraction (XRD). The depth-profile atomic concentration and ratio of nickel and other elements were evaluated by X-ray photoelectron spectroscopy (XPS) (ESCA Model SSX-100).

(19) Xiao, Z. G. *Rev. Sci. Instrum.* **2003**, *74*(8), 3879.

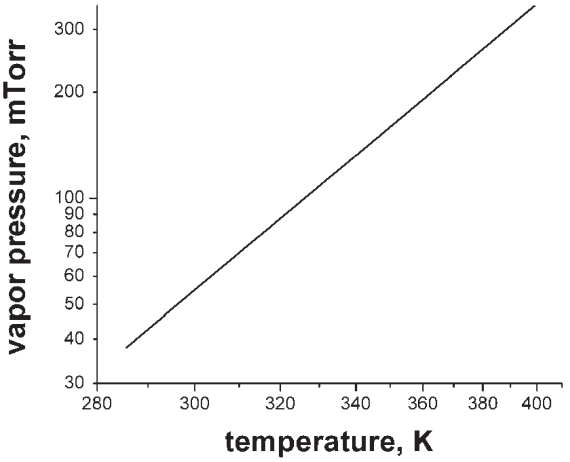

Figure 2. Vapor pressure of nickel bis(*N*,*N*′-di-*tert*-butylacetamidinate).

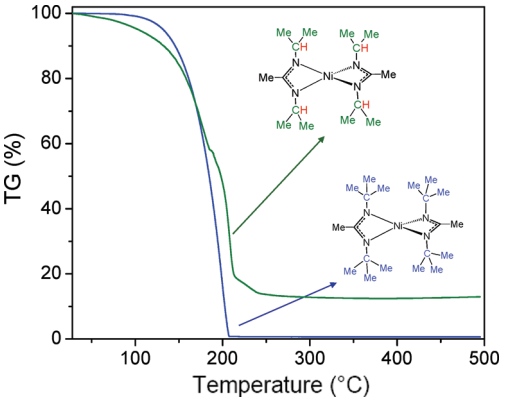

Figure 3. TGA curves of nickel bis(*N*,*N*′-di-*tert*-butylacetamidinate), nickel bis(*N*,*N*′-di-*iso*-propylacetamidinate), and nickel bis(*N*-*tert*-butyl-*N*′-ethylacetamidinate).

The surface roughness of the films was evaluated by atomic force microscopy (AFM) (Asylum Model MFP-3D AFM system).

Results and Discussion

Precursor Properties and Vaporization. The nickel precursor, bis(*N*,*N*′-di-*tert*-butylacetamidinato)nickel(II), is a dark brown, air-sensitive crystalline solid that melts at a temperature of 87 °C. This liquid precursor has a vapor pressure of ~200 mTorr at 90 °C and ~320 mTorr at 120 °C. The vapor pressure can be fit to the equation

$$\log(P,\ \text{mTorr}) = 1.977 - \frac{971}{T}$$

which is plotted in Figure 2. Thermogravimetric analysis (TGA) (see Figure 3) of $Ni(MeC(N^tBu)_2)_2$ confirmed the high volatility and showed excellent thermal stability (< 1% residue) of $Ni(MeC(N^tBu)_2)_2$ for time-scales of minutes up to 200 °C, by which temperature the precursor had completely vaporized. In contrast, the previously used nickel precursor, bis(*N*,*N*′-diisopropylacetamidinato)nickel(II)

(20) (a) Wu, J.; Li, J.; Zhou, C.; Lei, X.; Gaffney, T.; Norman, J. A. T.; Li, Z.; Gordon, R. G.; Chen, H. *Organometallics* **2007**, *26*, 2803. (b) Li, J.; Wu, J.; Zhou, C.; Han, B.; Lei, X.; Gordon, R. G.; Cheng, H. *Int. J. Quantum Chem.* **2009**, *109*, 756.

$(Ni(MeC(N^iPr)_2)_2)$, left a high TGA residue (>12%), because of poor thermal stability (see Figure 3). Theoretical calculations have identified a facile β-hydrogen decomposition pathway in the less-stable precursor.[20]

Studies of the thermal decomposition of $Ni(MeC(N^tBu)_2)_2$ were conducted by heating the neat liquid precursor in a sealed glass tube for 6 days at 150 °C. After dissolving it in C_6D_6 and NMR analysis, 18±2% of the material was determined to have decomposed. Accelerated Rate Calorimetry (ARC) measurements (see Figure 4) showed a pressure increase within an hour at 220 °C, which indicated significant thermal decomposition of the liquid at 220 °C in 1 h. For the DLI vaporization of the precursor solution, a temperature of 150 °C was chosen, because the solution evaporates completely and very quickly at this temperature. Tests at 120 °C indicated incomplete evaporation, so this temperature is too low for our DLI system. No decomposition products were found in the DLI system after months of operation at 150 °C, because the precursor is heated to this temperature for only a fraction of a second before it vaporizes and flows into the reactor.

Direct-Liquid-Injection Chemical Vapor Deposition (DLI-CVD) of Nickel Nitride. DLI-CVD of nickel, using the nickel precursor and molecular hydrogen (H_2) at 240 °C, leads to carbon in the films, as determined by depth-profile X-ray photoelectron spectroscopy (XPS) (not shown).

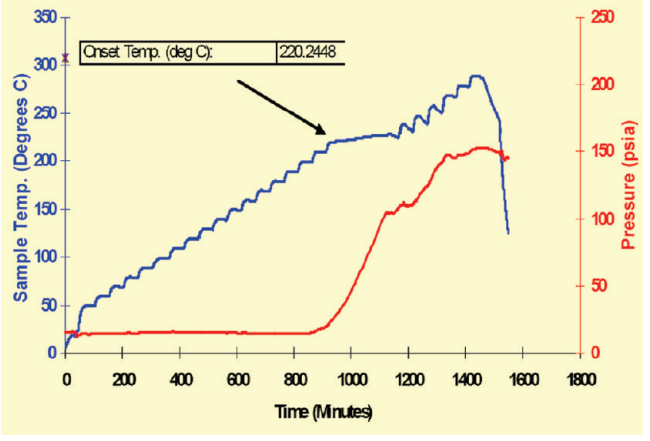

Figure 4. Accelerating Rate Calorimetry (ARC) measurement of the thermal stability of nickel bis(*N*,*N*′-di-*tert*-butylacetamidinate).

DLI-CVD of pure nickel, using H_2 as a co-reactant at 200 °C or lower temperatures, produced a very low growth rate (<0.5 nm/min).

When pure NH_3 was used as the co-reactant, the flow rate of NH_3 was 60 sccm, along with 60 sccm N_2 and a solution flow rate of 0.1 cm^3/min. The resulting partial pressures in the reactor at 200 °C are 0.12 Torr of the nickel precursor, 0.51 Torr of tetralin, 2.18 Torr of NH_3, and 2.18 Torr of N_2. The growth rate of NiN_x films deposited at a total pressure of 5 Torr and 200 °C was 3.6 nm/min, as determined by XRR (see Figure 5). The density of the as-deposited film was determined by combining the XRR thickness and the RBS areal density. For thin films (10−20 nm), the density of various samples was 6−7 g/cm^3, whereas for thicker films (50−60 nm), the density was 8−9 g/cm^3. The resistivity of the as-deposited NiN_x films deposited on thermally oxidized silicon wafers was 100 $\mu\Omega$ cm for films with thicknesses of ~40 nm, as shown in Figure 6. The AFM image (Figure 7a) showed that the rms roughness value (~2.5 nm) was ~10% of the total thickness (~25 nm) of the as-deposited NiN_x film. The Ni/N atomic ratio in NiN_x films deposited on glassy carbon was ~3, as determined by RBS (Figure 8). The depth-profile XPS (Figure 9a) obtained by argon-ion sputtering of NiN_x films from NH_3 shows that the Ni/N atomic ratio is ~3 and uniform throughout the film. On the other hand, the XPS analysis of NiN_x from a mixture of H_2 with a lower flow rate of NH_3, shown in Figure 9b, indicated a lower nitrogen content, particularly in the early stages of film

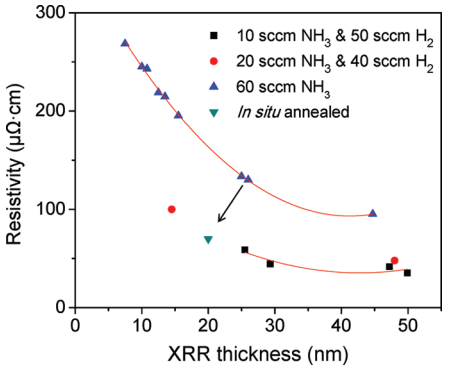

Figure 6. Resistivity of DLI-CVD films, as a function of XRR thickness.

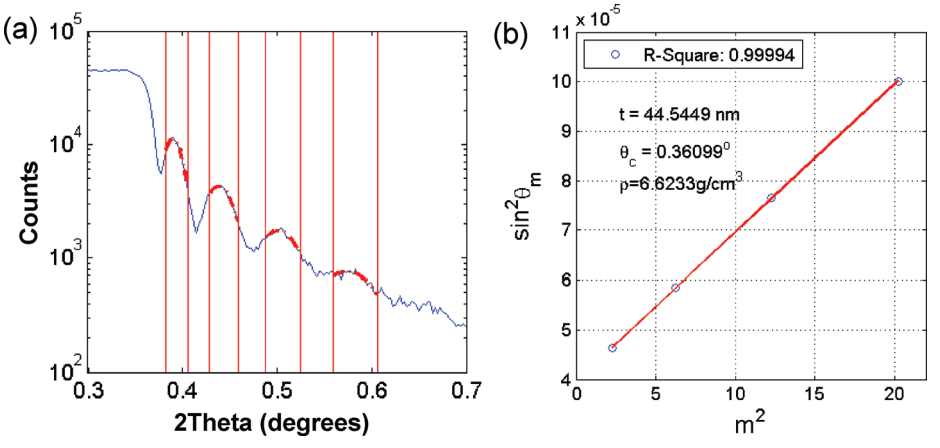

Figure 5. (a) XRR experimental curve and (b) fitted simulation line of a DLI-CVD NiN_x film deposited on silicon.

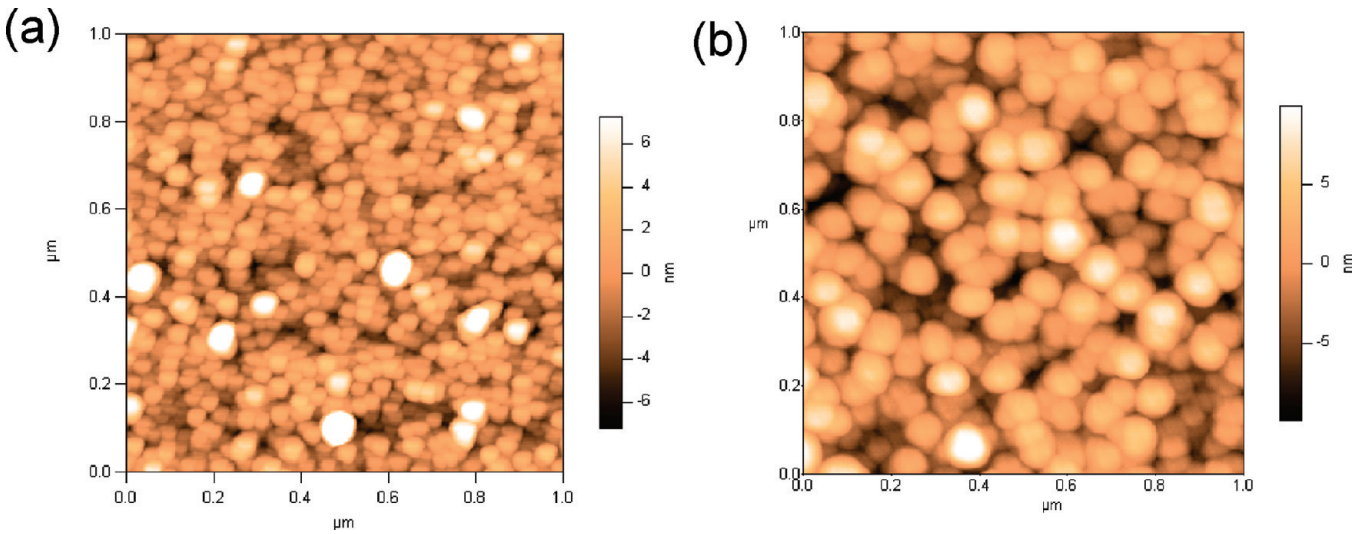

Figure 7. AFM images of (a) ~25-nm-thick DLI-CVD NiN_x film deposited with NH_3 on silicon (rms roughness = 2.521 nm); and (b) the film after in situ annealing in H_2 at 160 °C (rms roughness = 3.401 nm).

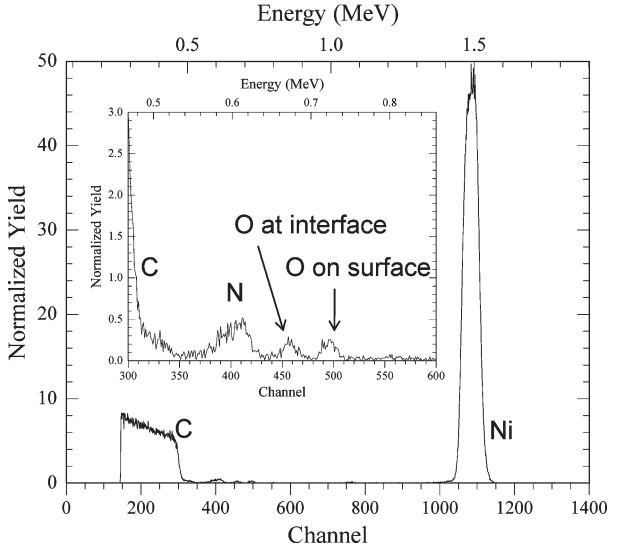

Figure 8. RBS spectra of DLI-CVD NiN_x films deposited from nickel bis(*N*,*N*′-di-*tert*-butylacetamidinate) and ammonia at 160 °C on a glassy carbon substrate.

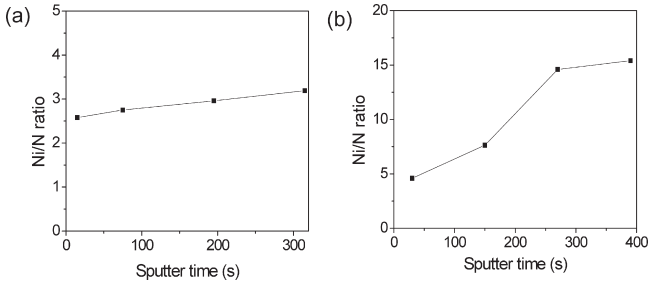

Figure 9. Ni/N atomic ratio obtained from depth-profile XPS, as a function of sputter time of the DLI-CVD NiN_x films deposited with (a) 10 sccm NH_3 and (b) 10 sccm NH_3 and 50 sccm H_2.

growth. Figure 10a shows the planar TEM image of a NiN_x film deposited on a Si_3N_4 membrane. The film is continuous, with a uniform grain size of ~5 nm. Electron diffraction (ED) (see Figure 10b) showed that the major diffraction peaks correspond to the hexagonal Ni_3N

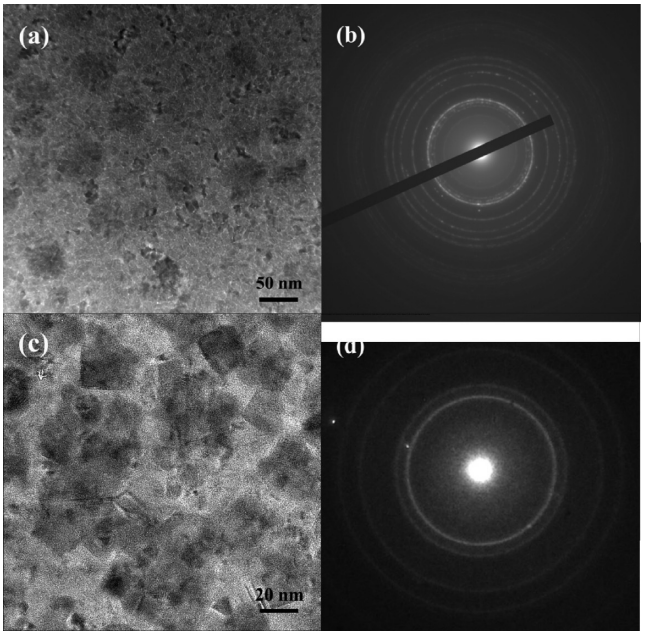

Figure 10. (a) TEM and (b) ED images of DLI-CVD NiN_x films deposited with 60 sccm NH_3 as a co-reactant; (c) TEM and (d) ED images of DLI-CVD NiN_x films deposited with 10 sccm NH_3 and 50 sccm H_2.

phase (PDF Card No. 70-9606), with smaller amounts of cubic Ni_4N (PDF Card No. 89-5145) (see Table 1). The bulk density of these phases is similar to the values measured for the thicker films.

The step coverage of the DLI-CVD NiN_x films was examined by depositing films on a silicon substrate that had holes with aspect ratios of > 50:1. It was found that, if the deposition pressure was as low as 1 Torr, the step coverage was nonuniform and, at most, ~70% step coverage could be achieved at the bottom. The step coverage increased as the deposition pressure increased. When the pressure was increased to 10 Torr, gas-phase reactions led to the formation of particles. The concentration of NH_3 was also determined to be an important factor affecting the step coverage. When the flow rate of NH_3 was 60 sccm, the step coverage was poor,

Table 1. Electron Diffraction (ED) Results for DLI-CVD NiN_x Film Using 60 sccm NH_3 as the Co-reactant[a]

	c-Ni_4N			*h*-Ni_3N				
No.	*hkl*	*d* (Å)	Int	*hkl*	*d* (Å)	Int	measured *d* (Å)	error[b] (%)
1	110	2.64	14				2.77	4.74
2	111	2.16	377	002	2.16	233	2.18	1.03
3				111	2.04	999	2.04	−0.03
4	200	1.87	577				1.93	3.21
5	210	1.67	258				1.71	3.24
6				112	1.58	151	1.49	−5.62
7	220	1.32	232	300	1.34	120	1.31	−1.03
8	221	1.25	80	113	1.22	104	1.26	0.97
9	311	1.13	57	302	1.14	84	1.15	1.19

[a] The indices of planes (*hkl*), interplanar spacings (*d*), and intensities (Int) shown in this table represent the reference crystal structures of Ni_4N (PDF Card No. 89-5145) and Ni_3N (PDF Card No. 70-9606). [b] Error means the difference between measured data and the closest reference data, expressed as a percentage.

because of the high growth rate of the films. Higher step coverage was found either by reducing the flow rate of NH_3 to 20 sccm or by decreasing the deposition temperature to 160 °C. A higher flow rate of the nickel precursor solution also increased the step coverage. The SEM image of a cleaved cross section in Figure 11 showed ~100% step coverage of the films deposited with 20 sccm NH_3, 100 sccm N_2, and 0.1 cm^3/min solution flow at 5 Torr at 200 °C. Energy-dispersive X-ray spectroscopy (EDAX) (not shown) confirmed that the films contained similar amounts of nickel all along the sides of the holes. These results demonstrate that excellent conformality can be achieved by the DLI-CVD method. The growth rate of the Ni_xN films under these conditions is 0.9 nm/min.

When a mixture of NH_3 (10 sccm) and H_2 (50 sccm) was used as the co-reactant, the growth rate of NiN_x films deposited at 200 °C increased to 5 nm/min. The density of an as-deposited film 50 nm thick was determined to be 8 g/cm^3 by combining the XRR thickness and RBS areal density. This film density is ~90% of the value for single-crystal nickel. Compared to films of similar physical thickness deposited using pure NH_3, the resistivity of the as-deposited NiN_x films using the mixture of NH_3/H_2 gases is significantly smaller and is ~50 $\mu\Omega$ cm for films with thicknesses of ~25 nm, as shown in Figure 6. The RBS spectra (not shown) of a NiN_x film deposited on glassy carbon showed that the N/Ni atomic ratio decreased to 0.09 when 50 sccm H_2, in addition to the 10 sccm NH_3 was added as a co-reactant. A depth-profile XPS of a film deposited on silicon confirmed that the addition of hydrogen during deposition reduced the nitrogen content of the films (see Figure 9b). This XPS also suggests that nitrogen may be inhomogeneously distributed inside the film, although this effect could be an artifact of the selective removal of nitrogen during sputtering. The nitrogen content of the as-deposited films was significantly lower than that of any known NiN_x phase. Figure 10c shows the planar TEM image of NiN_x film deposited using a mixture of NH_3/H_2 gases on a SiN membrane. The film contains several large rectangular crystallites with a diameter of ~20 nm. The ED analysis (Figure 10d) showed that the major diffraction peaks correspond to the known cubic nickel phase (PDF Card No. 01-1258) (see Table 2). These results indicated that the films

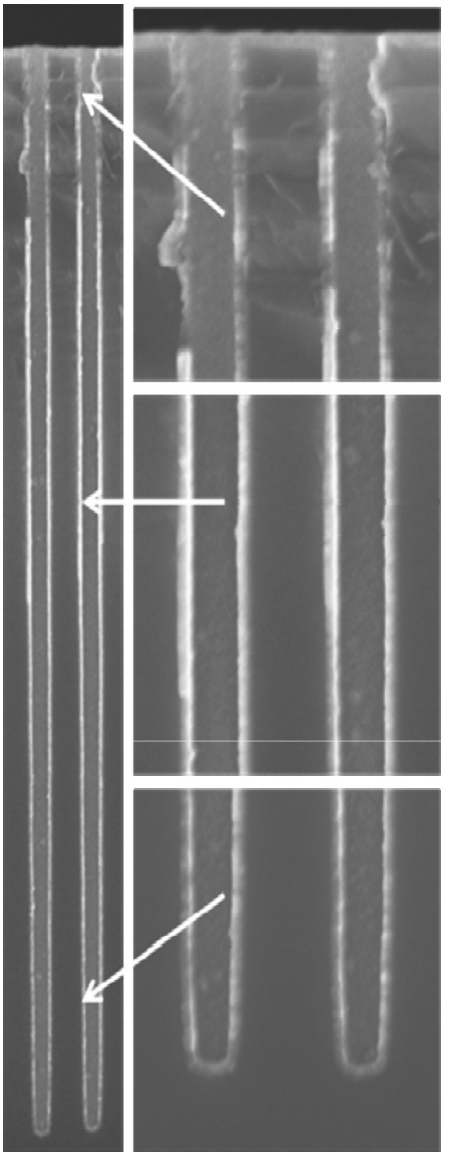

Figure 11. Cross-sectional SEM images of holes with 100 nm semilong axes, 55 nm semishort axes, and a depth of ~7.3 μm in a silicon wafer uniformly coated with ~35-nm-thick DLI-CVD NiN_x films deposited at 200 °C.

deposited with 10 sccm NH_3 and 50 sccm H_2 are mainly composed of cubic nickel crystallites incorporating a small amount of nitrogen. Depending on the ratio of NH_3 and H_2 gases flowing during deposition, the atomic percentage of nitrogen in the film could be as low as ~6 at. %.

Both nitrogen content and film thickness affect the resistivity of NiN_x films. The resistivity increases as the film thickness decreases, presumably because of scattering by grain boundaries (see Figure 6). Assuming that the grain size is comparable to the film thickness, the grain-boundary scattering effect predicts a linear increase of resistivity with inverse film thickness, as plotted in Figure 12 for films grown with three different concentrations of NH_3. Linear extrapolation of the points in Figure 12 to the *y*-axis gives the resistivity expected for thick films, which is plotted in Figure 13 as a function of nitrogen content (from RBS) in the films. If electron scattering by nitrogen adds to the phonon scattering already present in pure nickel (Matthiessen's rule), then the points in Figure 13 should lie on a straight line.

Table 2. ED Results for DLI-CVD NiN_x Film Using a Mixture of 10 sccm NH_3 and 50 sccm H_2 as the Co-reactant[a]

No.	*hkl*	*d* (Å)	Int	measured *d* (Å)	error[b] (%)
1	111	2.04	100	2.02	−0.76
2	200	1.77	50	1.74	−1.84
3	220	1.25	40	1.23	−1.45
4	311	1.07	60	1.05	−1.55

[a] The indices of planes (*hkl*), interplanar spacings (*d*), and intensities (Int) shown in this table represent the reference cubic nickel crystal structure (PDF Card No. 01-1258). [b] Error means the difference between measured data and the reference data, reported as a percentage.

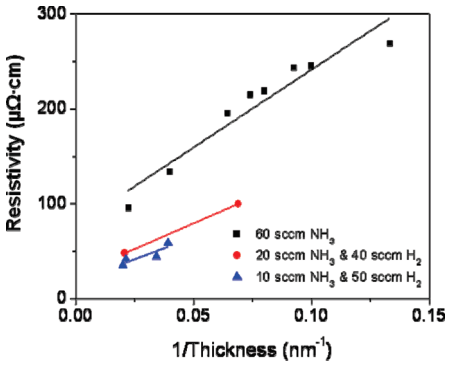

Figure 12. Resistivity of DLI-CVD NiN_x films, as a function of inverse XRR thickness. Black squares were deposited using 60 sccm NH_3; red circles using 20 sccm NH_3 and 40 sccm H_2; blue triangles using 10 sccm NH_3 and 50 sccm H_2.

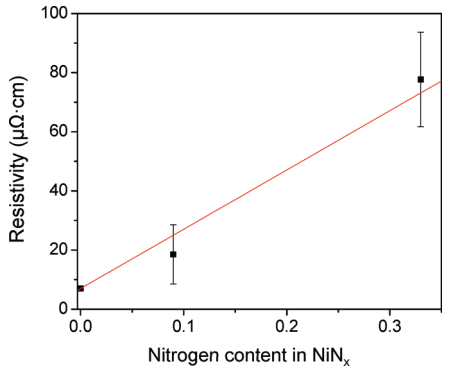

Figure 13. Expected resistivity for thick DLI-CVD NiN_x films, as a function of nitrogen content in NiN_x.

Within the experimental errors, this line describes the trend of increasing resistivity with increased nitrogen content.

It was determined that the films deposited on SiO_2 at 200 °C using a mixture of NH_3/H_2 gases were not continuous or conductive anymore when the film thickness was below ~20 nm, while the NiN_x films deposited at 200 °C using pure NH_3 remained continuous and conductive even if the film thickness was < 5 nm. Apparently, the NH_3 increases the nucleation density of the NiN_x films on SiO_2. To deposit thinner (< 10 nm) conductive NiN_x films with NH_3/H_2, the deposition temperature was decreased to 160 °C, which also reduced the deposition rate to ~1−2 nm/min.

As we see, H_2 was not reactive enough to reduce the nickel precursor quickly, while the deposition rate became much higher when some of the H_2 was replaced with NH_3. It appears that the DLI-CVD process employing a mixture of NH_3 and H_2 gases as the co-reactant may depend on two reactions: NH_3 first reacted with the nickel precursor and formed a nitrogen-rich nickel nitride Ni_3N, which subsequently reacted with H_2 to remove some of the nitrogen. Because of the reduced content of nitrogen, the density and electrical conductivity of the film became higher. Because the deposition happened very quickly, not all of the nitrogen reacted with hydrogen and desorbed from the surface, leaving several percent of nitrogen remaining in the films.

Reduction of Nickel Nitride Films to Metallic Nickel. The resistivity of the films could be further decreased by post-deposition in situ annealing with H_2 at 160 °C for 0.5−1 h, yielding pure nickel films without agglomeration, as indicated by lower sheet resistance from four-point-probe measurements. Room-temperature treatment of the as-deposited films with a remote H_2 plasma for 15 min yielded a similar reduction in resistance. Depth-profile XPS (not shown) indicated that no nitrogen was detected in these annealed nickel films. The AFM image (Figure 7b) showed that the rms roughness value increases slightly and the film was still continuous after annealing. For a nickel nitride film 26 nm thick deposited with NH_3 at 160 °C for 12 min, the resistivity was decreased from 130 $\mu\Omega$ cm to 70 $\mu\Omega$ cm after annealing (as shown in Figure 6), because of the removal of nitrogen and the increased density of the films. Compared to the resistivity of bulk nickel (7 $\mu\Omega$ cm), the resistivity of the annealed films is still high, which might be due to the low density (90%) of the films, compared to bulk nickel, the increased roughness of the films, and/or a trace amount of nitrogen incorporated in the films that was undetectable by XPS.

Another use of these NiN_x films is their reaction with silicon substrates to form nickel silicide (NiSi). This process is described in detail in another paper,[18] which shows that pure, fully dense, highly conductive, and smooth NiSi is formed without any nitrogen content.

Conclusions

Direct-liquid-injection chemical vapor deposition (DLI-CVD) processes employing our novel precursor, $Ni(MeC(N^tBu)_2)_2$, produced smooth and continuous NiN_x films with excellent step coverage in holes with aspect ratios of > 50:1. DLI-CVD NiN_x films have much higher growth rates than those grown via atomic layer deposition (ALD) processes. The growth rate of the DLI-CVD films was increased and the nitrogen content of the NiN_x films reduced by replacing part of NH_3 with H_2 during deposition. The remaining nitrogen in the films could be removed by post-annealing in H_2 or via room-temperature plasma treatment with H atoms.

Acknowledgment. We appreciate an NMR measurement of thermal decomposition by Dr. Wontae Noh. This work was performed, in part, at the Center for Nanoscale Systems (CNS), a member of the National Nanotechnology Infrastructure Network (NNIN), which is supported by the National Science Foundation (under NSF Award No. ECS-0335765). CNS is part of the Faculty of Arts and Sciences at Harvard University.